INTERNATIONAL JOURNAL OF OPTIMIZATION IN CIVIL ENGINEERING
Int. J. Optim. Civil Eng., 2015; 5(1):117-135

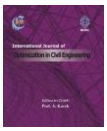

THREE SCHEMES FOR ACTIVE CONTROL OF THE PLANAR FRAME

M. Rezaiee-Pajand[*,†] and M. Payandeh Sani
Department of Civil Engineering, Ferdowsi University of Mashhad, Iran

ABSTRACT

Optimal locations of the actuators for frame active control are investigated in this article. The aim is to minimize the structural drifts by employing several actuators. By utilizing genetic algorithm, the appropriate locations of the actuators are determined. They should be placed in locations where they can minimize the maximum structural drift. To explore the capability of the proposed techniques, the response of a 20-story building is controlled using three suggested methods. Furthermore, two different concepts are considered for comparing the performance of the authors' approaches. One is based on the maximum responses of the structure, and the other is according to the magnitudes of the actuators' forces. All findings prove the efficiency of the recommended strategies.

Received: 15 September 2014; Accepted: 12 January 2015

KEY WORDS: active control; genetic algorithm; perception neural network; open loop; control; earthquake.

1. INTRODUCTION

Controlling the behavior of tall building is very common these days. This goal is achieved by changing the structural behaviors through applying forces to them. Recently, extensive studies have been carried out in the field of control engineering related to the earthquakes. All researches conducted in this area can be divided into two groups. The first category is devoted to the control devices. Since accuracy and sensitivity of required equipments play an important roll, some industries are trying to build better and more robust instruments. The key subject of the second group of researchers is developing new control algorithms.

The control methods can be classified into three categories. The first one is named

[*]Corresponding author: Department of Civil Engineering, Ferdowsi University of Mashhad, Iran
[†]E-mail address: rezaiee@um.ac.ir (M. Rezaiee-Pajand)

inactive structural control. In this system, there are no applied forces to the buildings. Undesired energy of the structure is suppressed in the inactive systems. To achieve this goal, the static or dynamic characteristics of the structures are altered. It is worth emphasizing; this tactic is not able to change the applied load pattern [1]. The second group is called semi-active control systems. These systems cannot insert mechanical energy into the structures. Nevertheless, some of their properties actively changed [2]. In semi-active control systems, forces are not applied to the structure by utilizing the outer source. In other words, the damping factors are actively adjusted based on the ground excitation. The last category is named active control system, which applies forces to the structures. It is worth mentioning; these forces are produced by employing the structural responses and ground vibrations. This strategy is more complicated in comparison with the other aforesaid tactics. The active control schemes require sensors and actuator devices. It should be added that the amount of produced forces and energy are limited in this approach [3]. Various types of algorithms are utilized in active control systems. Among them, genetic algorithms and neural networks are well-known and efficient. In 1995, Chen and Ghaboussi [4,5] deployed multilayer perceptron neural networks in active control systems, for the first time. Joghataie and Ghaboussi [4] have trained this neural network for seismic control of multi degrees of freedom structures. In this process, they utilized a fast method. The aforementioned tactic is faster than the training technique named error back propagation technique. Furthermore, Ghaboussi and Bani hani employed multilayer perceptron neural network in active control of nonlinear structures [6]. In the study of Ghaboussi *et al.*, the neural controller is trained in the group and out of line. Yang *et al.* [7] used neural networks in identification of patterns. Note that these investigators deployed multi-branch neural networks. This setup is a Perception neural network, and it is trained via error back propagation technique. It is worth emphasizing; the inputs of these networks are the history of the structural responses and ground acceleration. Since inputs affect the dynamic structural behavior in the various ways, and their properties are different; each of them enters a specific branch of the neural network. Kim et al. [8] have proposed a new neural network named probable network. They used this network in control systems. It is worth mentioning that the speed of these networks in training and prediction was more than previously introduced ones. Due to the importance of fastness in control of the structures, the usage of these systems has grown rapidly, and leads to the appropriate results. In probable networks, neurons are placed in four layers. Furthermore, they have proposed other types of probable networks [9]. For controlling structures, they have employed latticed and probable neural networks. The required computational efforts are reduced in this network. Hence, the aforesaid group is faster in comparison with the mentioned systems. Rezaeei-Pajand and Nikdel deployed multilayer perceptron neural networks to predict the appropriate force control. It should be added that they deployed the online system [10]. In their study, the ground acceleration was predicted by the neural network at each time step. Note that neural networks have extensively been applied in semi-active control of structures. Karamodin and Haji-Kazemi [11] and Han-Ja et al. [12] have done researches on the usage of neural networks in semi-active structural control. It is worth emphasizing that accuracy of the controllers, which use neural networks for simulation and prediction of the structural behavior and ground acceleration, are greatly dependent on the arrangement of the system and the training method. In fact, the amount of training is a key factor in simulation and prediction of the structural behavior.

In this paper, authors attempt to achieve more appropriate results in active control of structures by deploying several actuators. For this purpose, three new methods are suggested. The first proposed technique considers the force control for the actuator located in a story, equal to the shear force of that story. In the second scheme, the force control of each actuator is equal to the applied force of the actuated story in the first mode of the structure. In the third technique, the force control of each actuator is equal to the story force in which the actuator is placed. Note that the story force should be calculated based on the first mode of the structural vibration. In the third method, the force control of every actuator, which is placed in each story, is equaled to the load applied to that story. The open-loop control system is utilized in the present article.

It is worth emphasizing; perception neural network is used for predicting the ground acceleration. The number of each layer and its amount neurons are selected in a way that these factors lead to the minimum network's errors in predicting the ground acceleration of the next step. Four indices are considered to assess the capabilities of these tactics. These indicators are divided into two groups. The first set is utilized to evaluate the structural responses. By using the second category, the magnitude of the actuators' force control can be investigated. Herein, the ground acceleration is predicted by neural networks. Note that this network is trained out of the line. At the first stage, the optimum locations of the actuators are selected by using genetic algorithms. The location of the actuators should be chosen based on the ability to reduce the maximum lateral displacements in structures when earthquakes occur. To show the capability and weak-points of the proposed techniques, a 20-story building under several earthquakes is assessed. To investigate the merits of the suggested methods, this structure is equipped with various numbers of the actuators.

2. PREDICTION OF THE GROUND ACCELERATION

In this paper, Perception neural networks with several layers are deployed to predict the ground acceleration. In neural networks, neurons are the processing elements or units. They are connected via weighting matrices. In the training process of neural networks, the learned data are stored in these matrices. In this study, Levenberg-Marquardt method is applied for training the network. This strategy can converge rapidly. Due to this property, this scheme is extensively used in control of structures. In training process of neural network, the weights are modified until the criterion function is satisfied. At the current time step, the difference between the real ground acceleration and the acceleration predicted by the neural network constructs the criterion function of the neural network.

$$J = \frac{1}{2}(\hat{\ddot{u}}_g - \ddot{u}_g) \tag{1}$$

In this formula, the predicated acceleration by neural network and the real acceleration are denoted by $\hat{\ddot{u}}_g$ and $\ddot{u}_g$, respectively. It is worth mentioning; the perception network includes an input layer, one or several hidden layers and an output layer. The number of each selected layer's neurons should be able to maximize the efficiency of the network. Herein, the neural network is trained via El Centro and Northridge earthquake

accelerograms. Afterwards, the aforementioned network is capable of predicting the ground acceleration at the next step. The previous steps' earthquake accelerograms are the inputs of the neural network. It should be noted that the predicated acceleration is placed into the output layer. The accuracy of this layer in prediction of the acceleration plays an important role in performance of the control system. For this reason, several neural networks with various numbers of neurons are used. The error function has the subsequent shape:

$$E = \sum \left\| \ddot{u}_g(i) \right| - \left| \hat{\ddot{u}}_g(i) \right\| \tag{2}$$

In this equality, the error function is shown by E. Herein; neural networks with a different number of neurons are investigated. In control systems, the neural networks which produce fewer errors in the prediction process are applied. Several neural networks with their corresponding error functions are tabulated in Table 1.

Table1. Assessment of various neural networks to achieve the suitable arrangement

Number of neurons	E
15-13-10-7-1	147
15-15-8-7-1	151
15-14-12-5-1	162
15-9-9-4-1	183
15-11-11-11-1	205
15-12-11-10-1	221
15-15-14-4-1	233

The hidden layer's error of the neural networks depends on the number of neurons. The minimum error belongs to the network with the 1, 7, 10, 13, 15 neurons in hidden layer. As a result, these networks are deployed in a control system. To train the neural network, the acceleration records of El Centro and Northridge earthquake are used. The ten previous steps of the accelerograms data provide the required input of the network. In addition, the output is the acceleration of the earthquake which belongs to the coming step. Herein, Sigmoeid's function and linear function are applied in the intermediate and outer layer, respectively. Figs. 1 and 2 depict the capability of the neural network in the control system. In these figures, the predicted accelerations of the El Centro and Northridge earthquakes are compared with the exact values of these accelerations.

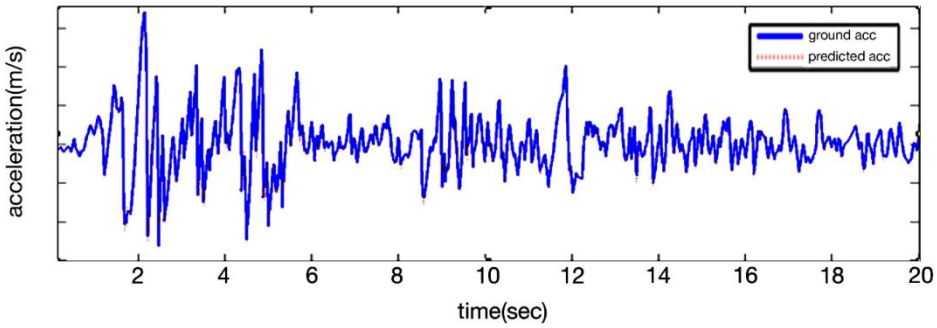

Figure 1. Comparison of the El Centro's predicted acceleration with the exact acceleration

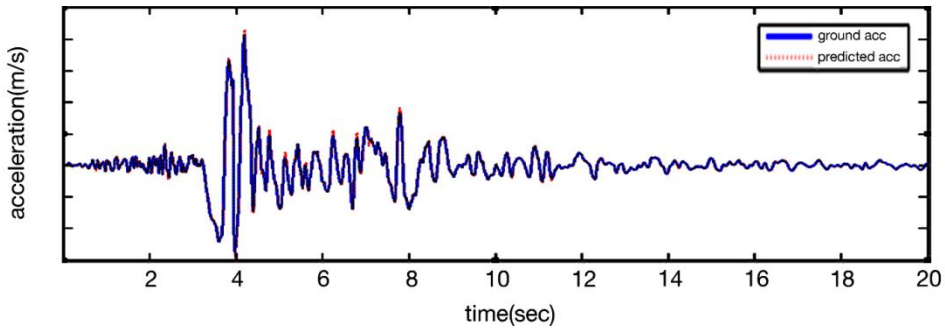

Figure 2. Comparison of the Northridge's predicted acceleration with the exact acceleration

3. DYNAMIC STRUCTURAL ANALYSIS

In this study, Newmark-Beta technique is employed to solve the structural differential equation of motion. This set of equation is solved numerically in each step. In each step, calculating the structural responses leads to achieving the force control of the succeeding steps. In 1959, Newmark proposed several numerical techniques for dynamic structural analysis. These approaches are based on the subsequent formulas [13]:

$$\dot{u}_{j+1} = \dot{u}_j + [(1-\gamma)\Delta t]\ddot{u}_j + (\gamma\Delta t)\ddot{u}_{j+1} \tag{3}$$

$$u_{j+1} = u_j + \Delta t\dot{u}_j + \left[(0.5-\beta)\Delta t^2\right]\ddot{u}_j + \left(\beta\Delta t^2\right)\ddot{u}_{j+1} \tag{4}$$

In these equalities, $\ddot{u}_{j+1}$, $\dot{u}_{j+1}$ and u_{j+1} denote the accelerations, velocities and displacements of the structures' stories, respectively. Time step is shown by Δt. Usually, the constant time step is used in the solution procedure. The change in acceleration of each step, stability properties and the accuracy of the aforesaid tactic are demonstrated by γ and β. It is worth emphasizing; γ and β are equal to 1/2 and 1/6, respectively, when it is assumed that the acceleration alters linearly in each step. By utilizing equation of motion

and equalities (3) and (4), u_{j+1} , $\dot{u}_{j+1}$ and $\ddot{u}_{j+1}$ can be obtained at the end of each step. Due to the existence of $\ddot{u}_{j+1}$ in the right side of equations (3) and (4), no iterative process is required to complete the analysis. In this paper, a linear behavior is presumed for the frame structures. In the linear systems, it is possible to simplify the Newmark's equation for analyzing without need to iterative process. For achieving this goal, the following formulas should be implemented:

$$\Delta u_i = u_{i+1} - u_i \tag{5}$$

$$\Delta \dot{u}_i = \dot{u}_{i+1} - \dot{u}_i \tag{6}$$

$$\Delta \ddot{u}_i = \ddot{u}_{i+1} - \ddot{u}_i \tag{7}$$

$$\Delta p_i = p_{i+1} - p_i \tag{8}$$

In these relations, changes in displacement, velocity, acceleration and force at the i-th step are shown by $\Delta u_i, \Delta \dot{u}_i, \Delta \ddot{u}_i$ and Δp_i , respectively. By deploying these equalities, the equation of motion and relationships (3) and (4) can be rewritten in the below form:

$$\Delta \ddot{u}_i = \left(\frac{1}{\beta(\Delta t)^2}\right)\Delta u_i - \left(\frac{1}{\beta(\Delta t)}\right)\dot{u}_i - \left(\frac{1}{2\beta}\right)\ddot{u}_i \tag{9}$$

$$\Delta \dot{u}_i = \left(\frac{\gamma}{\beta \Delta t}\right)\Delta u_i - \left(\frac{\gamma}{\beta}\right)\dot{u}_i - \Delta t\left(1 - \frac{\gamma}{2\beta}\right)\ddot{u}_i \tag{10}$$

$$m\Delta \ddot{u}_i + c\Delta \dot{u}_i + k\Delta u_i = \Delta p_i \tag{11}$$

With the help of these relations, changes in structural responses can be computed. It should be remarked; the structural responses can be achieved at the end of each time step by knowing their values at the beginning of the aforementioned time step.

4. PROPERTIES OF THE STRUCTURE

To assess the capability of the proposed techniques, they are employed in controlling of the 20-story structure [14]. It is assumed that all floors of the structure are rigid. As a result, each story includes a degree of freedom. Moreover, it is presumed that the material of the structure behaves linearly, during the earthquake.

5. INDICES ESTIMATION

In the proposed numerical samples, the structural responses are controlled by using various

numbers of actuators. To investigate the ability of the suggested control systems, the following indices are applied:

$$J_1 = \max\left\{\frac{\max_{t,i}\left|\frac{d_i(t)}{h_i}\right|}{\sigma_{\max}}\right\} \tag{12}$$

$$J_2 = \max\left\{\frac{\max_{t,i}\left|\ddot{x}_{ai}(t)\right|}{\ddot{x}_{\max}}\right\} \tag{13}$$

$$J_3 = \max\left\{\max_t \frac{\left|\sum_i m_i * \ddot{X}_{ai}(t)\right|}{F_b^{\max}}\right\} \tag{14}$$

$$J_4 = \max\left\{\max_{t,l} \frac{\left|f_l(t)\right|}{w}\right\} \tag{15}$$

J_1 index is based on the maximum drifts of the stories. In Eq. (12), $d_i(t)$ denotes the internal drift of the structure. Furthermore, $\sigma_{\max}$ is the maximum internal drift of the structure when the structural responses are not controlled. J_2 index is related to the maximum acceleration. At all steps, each story's acceleration of the controlled structure is demonstrated by $\ddot{x}_{ai}$. $\ddot{x}_{\max}$ denotes the maximum acceleration of the uncontrolled structure. In Eq. (14), the mass of the i-th story and the maximum acceleration of the uncontrolled structure are shown by m_i and $F_b^{\max}$, respectively. In addition, the force control of the l-th actuator and the structure's weight are f_l and *W, respectively.* J_1, J_2 and J_3 are dependent on the structural responses. On the other hand, J_4 denotes the maximum force control of the actuators.

6. PROPOSED TECHNIQUE

In this study, authors attempt to control the structural responses by using several actuators. Three methods are presented to determine the amount of forces applied to the structure by the actuators at each time step. The differences of these tactics are rooted in the approach used to create forces. Hence, the optimum locations of the actuators are different in each scheme. At first, genetic algorithm is deployed in each method to find the optimum locations of the actuators. If the actuators are located at the optimum places, the ratio of the maximum controlled structural drift to the uncontrolled one is minimized. At each time step, the force control is always applied to the structure in the direction opposite to the acceleration. It is obvious that employing this strategy decrease the applied force to the structure when the

earthquake occurs. Hence, the structural responses are reduced. It should be added that the ground acceleration is obtained by neural network at each time step. Clearly, the performance of the control system directly depends on the capability of the neural network.

6.1 First method

In this scheme, the force control of each actuator should be equal to the shear force of the story, which contains the actuator. The motion equation of multi-degree freedom structure has the coming appearance:

$$[m]\{\ddot{u}\}+[c]\{\dot{u}\}+[k]\{u\}=\{p(t)\} \tag{16}$$

In this formula, the mass matrix, damping matrix and stiffness matrix are demonstrated by $[m]$, $[c]$ and $[k]$, respectively. Acceleration, velocity and displacement vectors are $\{\ddot{u}\}$, $\{\dot{u}\}$ and $\{u\}$, respectively. Moreover, $\{p(t)\}$ denotes the vector of the external force applied to the structure. During the earthquake, the external force has the subsequent shape:

$$\{p(t)\}=-[m]\{I\}\ddot{u}_g \tag{17}$$

When the actuators are utilized in the structure, the equation of motion will change to the following one:

$$[m]\{\ddot{u}\}+[c]\{\dot{u}\}+[k]\{u\}=\{p(t)\}+\{f(t)\} \tag{18}$$

Here, the actuators' forces are shown by $\{f(t)\}$. Based on the fact that the actuator's force control of each time step is the shear force of the story, in which the actuator is placed, the succeeding relationship can be achieved:

$$f_i(t)=\sum_{j=i}^{20} m_j * \ddot{u}_g(t) \tag{19}$$

In this relation, the force control and the mass of the i-th story are f_i and m, respectively. In addition, $\ddot{u}_g$ denotes the earthquake's acceleration. Note that the neural network estimates the former acceleration at each time step.

6.2 Second procedure

In the second proposed strategy, the story's force control of the actuator equals the applied load to the story in the first structural vibration mode. The force control is in the direction opposite to the ground acceleration at each time step. It is well-known that the first mode of vibration plays an important role in the formation of structural responses. Hence, in the first mode of vibration, the responses are reduced by consuming the applied forces of several

stories. The distribution of the lateral loads based on the first mode of vibration has the next form:

$$m1 = \sum_{n=1}^{N} S_n = \sum_{n=1}^{N} \Gamma_n m \phi_n \tag{20}$$

In this equality, the number of vibrating modes and mass matrix are shown by N and m, respectively. By multiplying the mass matrix to a unit vector, the m1 vector is obtained. The natural mode shape of vibration corresponding to the nth mode is demonstrated by ϕ_n. Other parameters can be achieved by utilizing the succeeding relationships:

$$\Gamma_n = \frac{L_n^h}{m_n} \tag{21}$$

$$L_n^h = \sum_{j=1}^{N} m_j * \phi_{jn} \tag{22}$$

$$m_n = \sum_{j=1}^{N} m_j * \phi_{jn}^2 \tag{23}$$

Based on the former equations, the n-th mode's portion of mass vector is S_n vector. This vector denotes the distribution of mass in the height of the structure. It is worth emphasizing, the force control of each actuator is obtained by multiplying the earthquake's acceleration to the corresponding entry of the S_n vector.

6.3 Third technique

In this strategy, the force control of each actuator equals to the force applied to the story at each time step. This force is obtained by multiplying the earthquake acceleration by the mass of the story in which the actuator is placed. Using the following equation results in the force of each actuator:

$$f_i(t) = m_i * \ddot{u}_g(t) \tag{24}$$

In this relation, the force control and the mass of the i-th story are shown by f_i and m_i, respectively. This control force is applied to the structure by the actuator. Moreover, at each time step, the earthquake's acceleration is demonstrated by $\ddot{u}_g$.In the following sections, several numerical samples are presented to evaluate the robustness of recommended tactics. In these samples, three, four and five actuators are used to control the behavior of the structure. By this way, the effect of the number of actuators on the structural responses is investigated. At first, the optimum locations of the actuators are determined. The optimum locations are found by deploying the genetic algorithm. It should be noted; this algorithm is employed to minimize the J_1 index. In a process of minimizing the aforesaid index, the acceleration records of the El Centro earthquake are applied. Furthermore, it is assumed that

the neural network is able to accurately estimate the ground acceleration in the process of determining the optimum locations of actuators. Hence, no errors exist due to the incorrect prediction of the ground acceleration.

7. NUMERICAL STUDIES

7.1 First numerical study

In this example, three actuators are applied. By minimizing the index related to the displacements, the optimum locations of actuators are specified. Recall that the differences of the authors' techniques are rooted in the applied method for creation of the force control. The optimum placements of actuators are not similar. Table 2, presents the appropriate locations of actuators and the values of indices for each tactic.

Table 2: Optimum locations and values of control indices under the El Centro earthquake, when three actuators are used

Method	Optimal story location	**J1**	**J2**	**J3**
1	17-12-6	1.2442	2.6428	0.4261
2	4-3-2	0.7856	0.9130	0.9728
3	7-4-3	0.6149	0.9355	0.8447

It is presumed that the structure is subjected to the Northridge, El Centro and Kobe earthquake. In these situations, the neural network is employed in the control system. Then, the ground acceleration of the coming step is computed. The proposed approaches are deployed to create the force control. The values of the control indices are inserted in Table 3.

Table 3: Values of the control indices for the structure under the El Centro, Northridge, Hachinohe and kobe earthquake, when three actuators are applied

Method	earthquake	J1	J2	J3
1	El Centro	1.2892	2.7542	0.4315
	Kobe	0.9818	1.2287	0.2512
	Hachinohe	0.8322	1.8209	0.3461
	Northridge	1.0171	2.0887	0.2218
2	El Centro	0.7857	0.9154	0.9727
	Kobe	0.8507	0.8722	0.9766
	Hachinohe	0.8902	0.9118	0.9642
	Northridge	0.9028	0.8008	0.9529
3	El Centro	0.6208	0.9401	0.8447
	Kobe	0.6109	0.6603	0.8584
	Hachinohe	0.7401	0.8249	0.8662
	Northridge	0.7306	0.8362	0.8463

In the first suggested tactic, the indices related to the acceleration and drifts increase. On the other hand, the index associated with the shear force is considerably reduced. To assess

the structure's behavior in this situation, the first story's drift of the controlled and uncontrolled structure are depicted in Fig. 3.

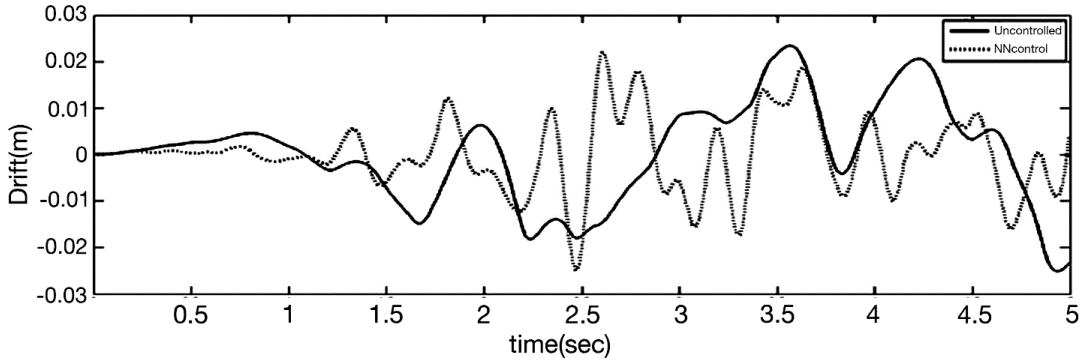

Figure 3. First story's drift of the controlled and uncontrolled structure, when the first technique is applied and three actuators are used

For the first five seconds of the El Centro earthquake, the former diagram is drawn. It is obvious that the direction of the structural displacement changes. Since the actuator forces have high values, the force control modifies the direction of the displacements. As a result, the shear force is reduced intensively. Moreover, the last actuator is placed in the 17-th story. Fig. 4 illustrates the displacement diagram of the 20-th story of the structure under the El Centro earthquake.

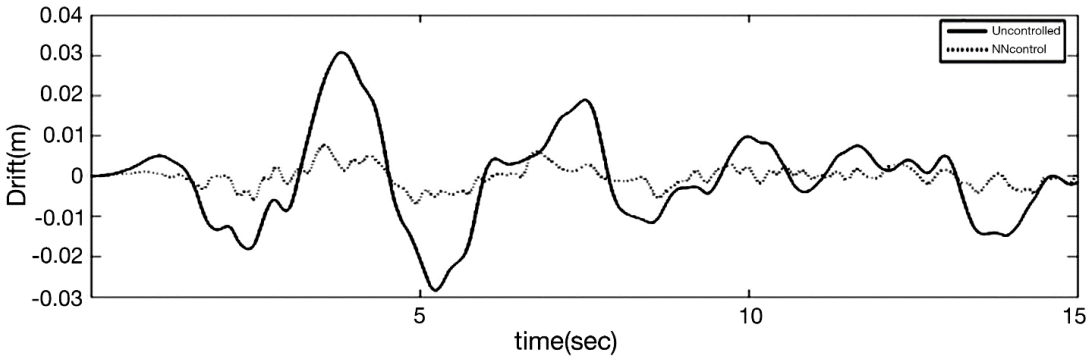

Figure 4. Displacement diagram of the 20-th story under the El Centro earthquake, when the first approach with three actuators is deployed

It is worth emphasizing; the structural displacement in the 20-th story is reduced considerably. The absolute values of 20-th story's displacements in controlled and uncontrolled structure are 0.0766 and 0.3067, respectively. Based on Table 3, it is obvious that the second and third method perform more properly, in comparison with the first tactic. Additionally, the maximum acceleration and drift index are reduced. Figs. 5 and 6 show the first story's drift of the controlled and uncontrolled structure under the El Centro earthquake, respectively. To create the force control, the second and third techniques are used in Figs. 5 and 6, respectively.

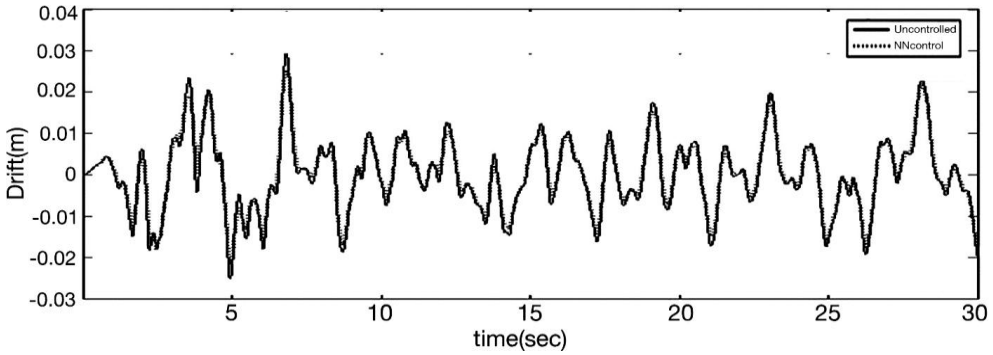

Figure 5. First story's drift in controlled and uncontrolled structure under El Centro earthquake, when the second approach is employed

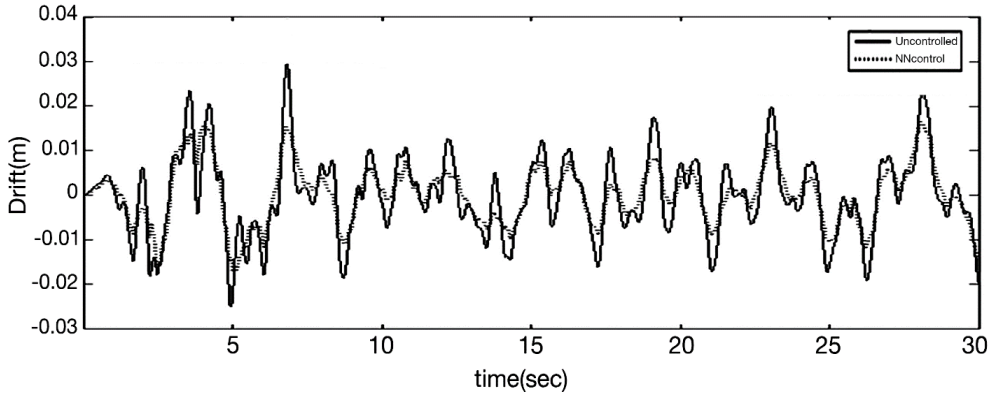

Figure 6. First story's drift in controlled and uncontrolled structure under El Centro earthquake, when the second approach is employed

Obviously, the force control does not change the direction of displacement when the second and third methods are deployed. Hence, when three actuators are used, the third tactic is more efficient, in comparison with other approaches.

7.2 Second numerical test

Four actuators are utilized in this test. At first, the optimum locations of actuators are specified for all tactics. It should be reminded; genetic algorithm and accelograms of El Centro earthquake are deployed to determine the actuators' locations. Table 4 shows the optimum placements of actuators.

Table 4: Optimum location of actuators and the values of control indices under El Centro earthquake, when four actuators are used

Method	Optimum story location	J1	J2	J3
1	18-14-9-4	0.7167	2.297	0.151
2	5-4-3-2	0.7388	0.9019	0.9492
3	9-4-3-2	0.53	0.7203	0.8165

Subsequent to determination of the actuators' locations, they are placed in stories. Afterwards, El Centro, Northridge, Kobe and Hachinohe earthquake are applied to the structure. The control indices are tabulated in Table 5.

Table 5: Control indices under El Centro, Northridge, Kobe and Hachinohe earthquake, when four actuators are deployed

Method	Earthquake	J1	J2	J3
1	El Centro	0.7484	2.3230	0.2196
	Kobe	0.4561	0.6932	0.1809
	Hachinohe	0.4658	1.484	0.1362
	Northridge	0.5566	1.3869	0.1579
2	El Centro	0.7391	0.9059	0.9492
	Kobe	0.8010	0.8267	0.9564
	Hachinohe	0.8568	0.9404	0.9446
	Northridge	0.8758	0.8008	0.9529
3	El Centro	0.5362	0.7198	0.8158
	Kobe	0.5735	0.5884	0.8366
	Hachinohe	0.7104	0.8801	0.8138
	Northridge	0.6628	0.7671	0.829

Clearly, the control index related to the maximum acceleration increases in the first method. However, the base acceleration and maximum drift index are considerably reduced. This method is applied to the control system. Then, the obtained responses are compared with the uncontrolled structure’s responses to investigate the structural behavior. The results are shown in Fig. 7.

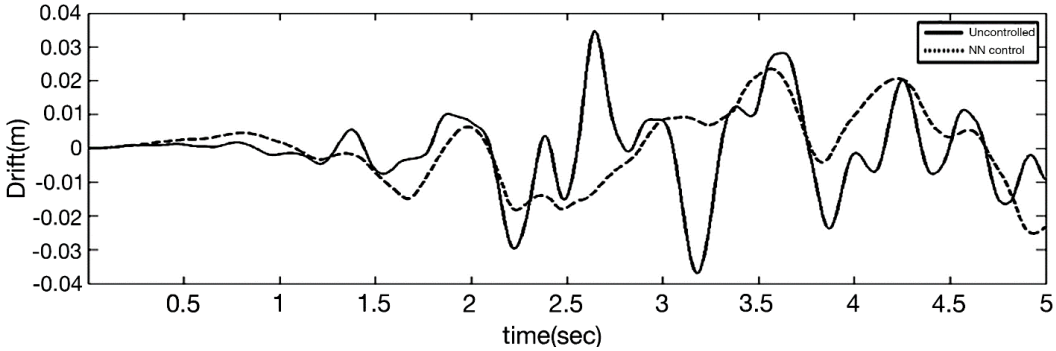

Figure 7. Diagram of the first story’s drift under the El Centro earthquake, when four actuators are used

Based on this figure, it is clear that the direction of the displacements is altered. As a result, the acceleration index increases. When the second and third tactics are employed, the first story’ displacement under El Centro earthquake are calculated. The obtained results are compared with the uncontrolled structural responses in Figs. 8 and 9.

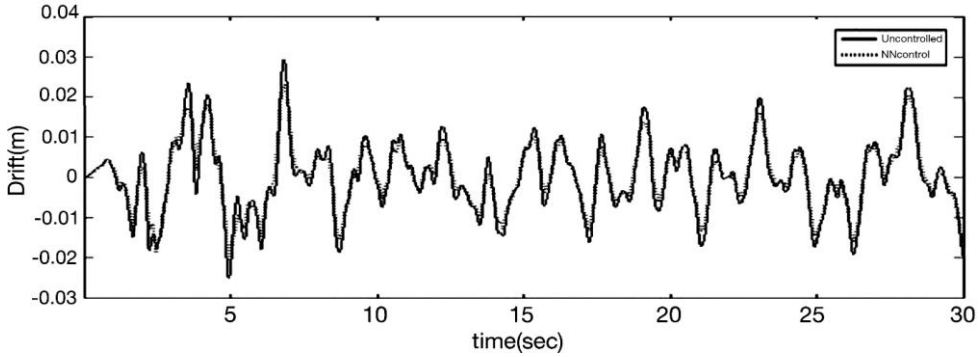

Figure 8. Diagram of the first story's drift under the El Centro earthquake, when four actuators and the second method are employed

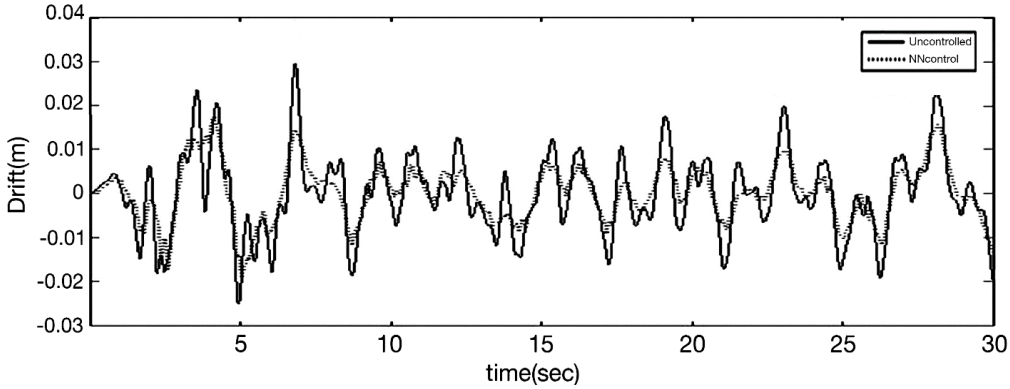

Figure 9. Diagram of the first story's drift under the El Centro earthquake, when four actuators and the third method are employed

It is obvious that the direction of the displacement does not change when the second and third methods are used. By comparing Tables 3 and 5, it can be deduced that increasing the number of actuators causes the responses to be reduced in all tactics.

7.3 Third numerical sample

In this section, five actuators are deployed for controlling the structure. At first, the optimum locations of actuators are determined for each method. To achieve this purpose, the displacement index is minimized by using genetic algorithm. To find the optimum location of actuators, the structure is subjected to the El Centro earthquake. The optimum locations of actuators and the values of indices are inserted in Table 6.

Table 6: Optimum locations of actuators and the control indices under El Centro earthquake, when five actuators are deployed

Method	Optimum story location	J1	J2	J3
1	19-17-14-9-4	0.5017	2.1485	0.1733
2	5-4-3-2-1	0.7284	0.8749	0.9482
3	9-6-4-3-2	0.4989	0.6309	0.7486

In each technique, the actuators' locations are specified based on the former Table. Then, the accelerograms of El Centro, Northridge, Kobe and Hachinohe earthquake are used. Note that neural network is applied to the control system. The corresponding control indices are illustrated in Table 7.

Table 7: Control indices under El Centro, Northridge, Kobe and Hachinohe earthquake, when five actuators are utilized

Method	Earthquake	J1	J2	J3
1	El Centro	0.5306	2.1777	0.26
	Kobe	0.4268	0.5894	0.1337
	Hachinohe	0.3938	1.3785	0.1536
	Northridge	0.4721	1.1844	0.161
2	El Centro	0.7286	0.8776	0.9481
	Kobe	0.7971	0.8171	0.9553
	Hachinohe	0.8533	0.9261	0.9429
	Northridge	0.8696	0.7489	0.9246
3	El Centro	0.5048	0.6208	0.7481
	Kobe	0.4533	0.4847	0.7741
	Hachinohe	0.6565	0.7346	0.776
	Northridge	0.5622	0.7089	0.7759

In the first scheme, the control index related to the maximum acceleration is increased. Nevertheless, the base acceleration and maximum drift indices are considerably reduced. Based on previously mentioned samples, it is predicted that the directions of the displacements are changed. Note that the force control of each story is equal to the shear force of the corresponding story. When the first method is used, the first story's drift of the controlled and uncontrolled structure are compared.

Based on Fig. 10, it is obvious that acceleration index is increasing. High force control can change the direction of the displacement. By using the second and third techniques, the first story's drift of the controlled and uncontrolled structure for the El Centro earthquake are obtained. Figs. 11 and 12 demonstrate the results of the second and third tactics, respectively.

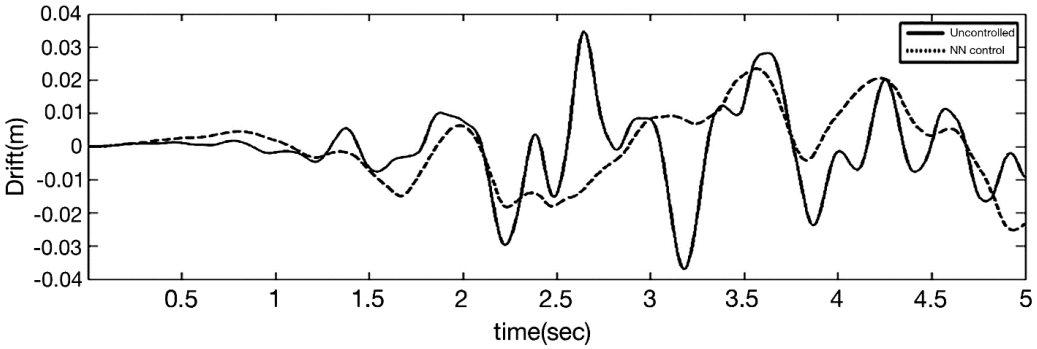

Figure 10. Diagram of the first story's drift under the El Cento earthquake, when the first tactic and five actuators are used

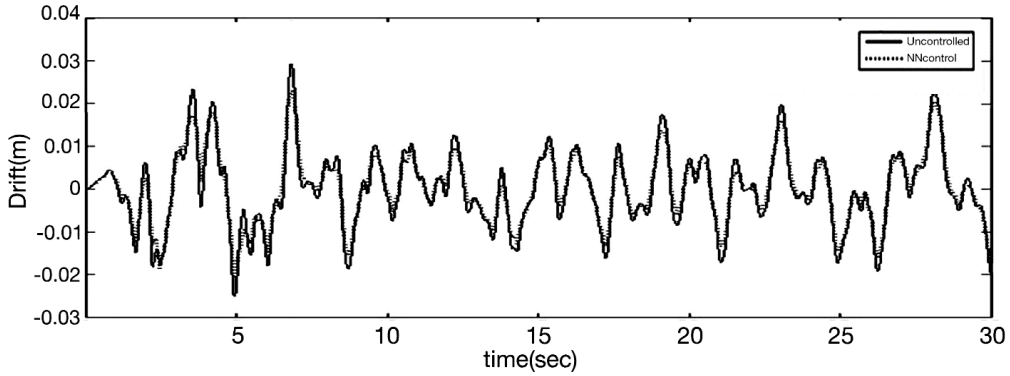

Figure 11. First story's drift for the El Centro earthquake, when the second method and five actuators are applied

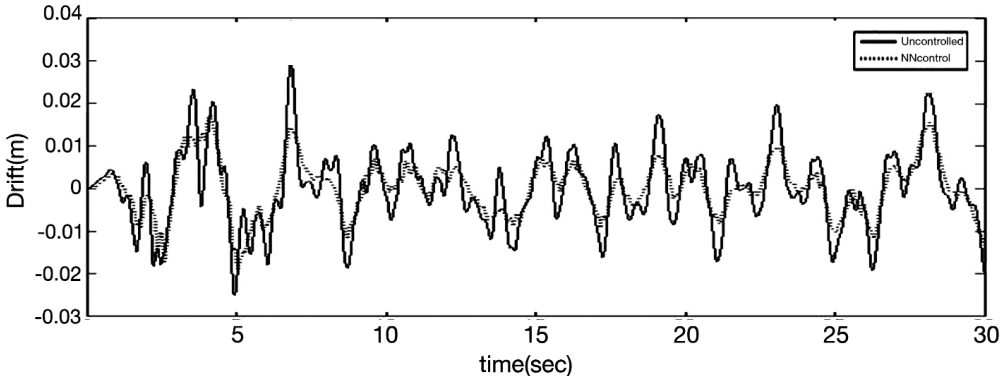

Figure 12. First story's drift under the El Centro earthquake, when the third method and five actuators are applied

It is obvious that the direction of the stories' displacements do not change, when the second and third approaches are utilized. In fact, the only factor which resists against displacement is the force control. Note that, the damage occurred in the structures are directly related to the frames' drifts during the earthquake. The acceleration, which is induced by the earthquake, discomforts the occupants. Keeping in mind, damage occurred in structures are more crucial than the comforts of the occupants. Hence, the first proposed

technique is more efficient in controlling of the frames.

8. MAXIMUM ACTUATORS' FORCES

In active control of structures, the outer source provides the force control. Therefore, minimizing the aforesaid force leads to the economical design. To compare the suggested techniques based on this issue, another index is presented. This new index evaluates the maximum force control of the actuators. The former index is introduced in the following form:

$$J_4 = \max\left\{\max_{t,l} \frac{|f_l(t)|}{w}\right\} \tag{15}$$

For the El Centro, Kobe, Northridge and Hachinohe, the maximum force control of actuators and the corresponding values of the aforementioned index are inserted in Table 8-10.

Table 8: Force control index by deploying three actuators in the frame

Earthquake	First method		Second method		Third method	
	Maximum force control *(N)*	J_4	Maximum force control *(N)*	J_4	Maximum force control *(N)*	J_4
El centro	5702700	0.104963	316730	0.00583	950460	0.01749
Hachinohe	4100000	0.075464	227970	0.004196	684100	0.012591
Kobe	13437000	0.263203	746310	0.013736	2239600	0.041222
Northridge	14300000	0.263203	749220	0.01379	2383300	0.043867

Table 9: Force control index by deploying four actuators in the frame

Third method	First method		Second method		Third method	
	Maximum force control *(N)*	J_4	Maximum force control *(N)*	J_4	Maximum force control *(N)*	J_4
El centro	5227500	0.09622	354309	0.00652	950473	0.01749
Hachinohe	3760250	0.06921	255049	0.00469	6841958	0.12593
Kobe	12317500	0.22672	834417	0.01536	2239843	0.04123
Northridge	13108500	0.24127	5285370	0.09728	2383319	0.04387

Table 10: Force control index by deploying five actuators in the frame

Earthquake	First method		second method		third method	
	maximum force control (N)	J4	maximum force control (N)	J4	maximum force control (N)	J4
El centro	4752300	0.08747	391710	0.00721	950598.84	0.01750
Hachinohe	3420500	0.06296	281930	0.00519	684254.44	0.01259
Kobe	11198000	0.20611	922980	0.01699	2239244.3	0.04122
Northridge	11917000	0.21934	9822300	0.01808	2382691.6	0.04386

Based on these tables, the force control by the first method is more suitable, in

comparison to the other tactics. When five actuators are applied, this force equals 4752300 N. It is worth emphasizing; this value is 12 and 5 times of the required force in the second and third approaches, respectively. In fact, the required force for controlling the structure is more than the other techniques. Nevertheless, this strategy is more capable of reducing the drifts, in comparison with the other methods. To produce such a huge force, hydraulic actuators can be employed. These actuators are able to produce the forces with the magnitude of 10^8 N [15-16].

9. CONCLUSIONS

The main focus of this study was on the appropriate use of actuators in the active control of structures. In the present article, the open-loop control system was utilized. The ground acceleration was predicted by neural networks. By employing genetic algorithm, the actuators were placed in locations to minimize the maximum structural drift. In order to reach this goal, three methods were proposed. The first suggested technique considered the force control for the actuator located in a story, equal to the shear force of that story. In the second scheme, the force control of each actuator was equal to the applied force of the actuated story in the first structural mode. In the third technique, the force control of each actuator was equal to force of the story in which the actuator was placed. The story force was calculated based on the first mode of the structural vibration. In the third method, the force control of each actuator was equaled to the load applied to that story.

The optimal location of the actuators was chosen based on the ability to reduce the maximum lateral displacements in structures when earthquakes occur. To show the capability and weak-points of the proposed techniques, a 20-story building under several earthquakes was evaluated. To investigate the merits of the suggested methods, this structure was equipped with various numbers of the actuators. Numerical studies clearly demonstrated the efficiency of the authors' strategies.

REFERENCES

1. Connor J. *Introduction to Motion on Control*, Massachusetts Institute of Technology, Boston, 2000.
2. Sepencer Jr BF, Sain MK. Controlling buillding: a new frontier in feedback, *Special Issue of the IEEE Control Sys Mag Emerging Technol* 1997; **17**: 19-35.
3. Kerber F, Hurlebaus S, Beadle BM, Stobener U. Control concepts for an active vibration isolation system, *Mech Syst Signal Process* 2007; **21**: 3042-59.
4. Ghaboussi J, Joghataei A. Active control of structures using neural networks, *J Eng Mech* 1995; **121**: 555-67.
5. Chen HM, Tsai KH, Qi GZ, Yang JCS, Amini F. Neural network for structure control, *J Comput Civil Eng* 1995; **9**: 168-76.
6. Bani-Hani K, GHaboussi J. Nonlinear structure control using neural networks, *J Eng Mech* 1998; **124**: 319-27.

7. Li H, Yang H. System identification of dynamic structurs by the multi-branch BPNN, *Neurcomputing* 2007; **70**: 835-41.
8. Kim DK, Lee JJ, Chang SK. Active vibration control of a structure using probabilistic neural network, *86th Annual Meeting*, Washington, DC, February 2007.
9. Dong yawn K, Dookie K, Seongkyu Ch, Hie-Young J. Active control strategy of structures based on lattice type probabilistic neural network, *Prob Eng Mech* 2008; **23**: 45-50.
10. Rezaiee-Pajand M, Akbarzadeh-T MR, Nikdel A. direct adaptive neurocontrol of structures under earth vibration, *J Comput Civil Eng, ASCE* 2009; **23**: 299-307.
11. Karamodin A, H-Kazemi H. Semi-active control of structures using neuro-predictive algorithm for mr dampers, *Struct Control Health Monit* 2010; **17**, 237-53.
12. Heon-jae L, Guangqiang Y, Hyung-Jo J, Spencer Jr Billie F, In-Won L. Semi-active neurocontrol of a base-isolated benchmark structure struct, *Control Health Monit* 2006; **13**: 682-92.
13. Anil K Chopra. *Dynamics of Structures, Theory and Aplications to Earthquake Engineering*, Pearson Prentice Hall, Third edition, Califirnia, 2007.
14. Ohtori Y Christenson, Spenser RE, BF Jr, Dyke SJ. Benchmark control problems for seismically excited nonlinear buildings, *J Eng Mech* 2004; **130**: 366-87.
15. Aaron S Brown, Henry TY Y. Neural networks for multiobjective adaptive structural control, *J Struct Eng* 2001; **127**: 0203-10.
16. Dorey AP, Moore JH. *Advances in Actuators*, Institute of Physics Publishing, 1995.